ELSEVIER

J. Non-Newtonian Fluid Mech. 125 (2005) 143–158

Journal of Non-Newtonian Fluid Mechanics

www.elsevier.com/locate/jnnfm

Stability of two-layer viscoelastic plane Couette flow past a deformable solid layer: implications of fluid viscosity stratification

V. Shankar*

Department of Chemical Engineering, Indian Institute of Technology, Kanpur 208016, India

Received 7 May 2004; received in revised form 10 October 2004; accepted 4 November 2004

Abstract

The linear stability of two-layer plane Couette flow of upper-convected Maxwell (UCM) fluids of thicknesses $(1-\beta)R$ and βR, with viscosities μ_a and μ_b, and relaxation times τ_a and τ_b past a linear viscoelastic solid layer (of thickness HR, shear modulus G, and viscosity η_w) is determined using a combination of low wavenumber asymptotic analysis and a numerical method. The asymptotic analysis is used to determine the effect of the deformable solid layer on the two-fluid interfacial instability due to elasticity and viscosity stratification in the low wavenumber limit. The asymptotic results show that as the solid layer is made more deformable, the two-fluid interfacial instability could be completely stabilized in the long wave limit, when the non-dimensional parameter $\Gamma = V\mu_b/(GR) \sim O(1)$ exceeds a certain critical value. Here, V is the dimensional velocity of the moving top plate. In marked contrast with the previous results obtained for matched fluid viscosities [V. Shankar, J. Non-Newtonian Fluid Mech., 117 (2004) 163], the present asymptotic results show that the stabilizing or destabilizing nature of the solid layer on the two-fluid interfacial instability is controlled *only* by the fluid viscosity ratio and is independent of the relaxation times of the two UCM fluids. In general, it is found that the solid layer has a stabilizing effect for $\beta < 0.5$, $\mu_r < 1$ and $\beta > 0.5$, $\mu_r > 1$, while it has both stabilizing and destabilizing effects (depending on its thickness H, and the fluid thickness ratio β) for $\beta > 0.5$, $\mu_r < 1$ and $\beta < 0.5$, $\mu_r > 1$. In the absence of the solid layer, the two-fluid interfacial mode is unstable or stable depending on the ratio of relaxation times between the two fluids and the thickness ratio β. It is thus possible, under appropriate combinations of relaxation times, viscosities, and thicknesses of the two fluids, to stabilize (destabilize) the two-fluid interfacial mode by the deformable solid layer while it is unstable (stable) in the absence of the solid layer. Another important result from the present low wavenumber (denoted by k) analysis is that the non-dimensional solid elasticity parameter Γ required to stabilize or destabilize the two-fluid interfacial mode is an $O(1)$ quantity in the low-k-limit when $\mu_a \neq \mu_b$, with numerical values of Γ significantly smaller than 1 for $H \sim O(1)$. Whereas when $\mu_a = \mu_b$ our asymptotic analysis (as well as the earlier study) shows that $\Gamma \propto k^{-1}$ for $k \ll 1$. The results from the low-k-asymptotic analysis are continued numerically to finite values of k and Reynolds number, and the numerical results confirm that the stabilization of the two-fluid interfacial mode by the solid layer extends to finite values of k. However, for short wavelength fluctuations with $k \gg 1$, the fluid velocity perturbations are localized near the two-fluid interface, so the solid layer has no effect on these fluctuations. These short wavelength unstable modes can be stabilized only by the presence of a sufficiently strong interfacial tension between the two fluids. Thus, the present study shows that the viscosity mismatch between the two fluids profoundly changes the stabilizing or destabilizing effect of the deformable solid layer on the two-fluid interfacial mode in viscoelastic fluids when compared to the conclusions reached using matched fluid viscosities.

Keywords: Interfacial instability; Viscoelastic fluids; Two-layer flows; Linear stability analysis; Low wavenumber analysis

1. Introduction

The study of interfacial instabilities in two-layer and three-layer flows of viscoelastic fluids has been an extensive area of research in the recent past [1–12], and these studies have identified (both by theoretical and experimental means) the presence of qualitatively new interfacial instabilities in viscoelastic fluids that are absent in Newtonian fluids. A clear understanding of such instabilities could be of relevance to polymer processing applications, such as multi-layer extrusion, where an accurate knowledge of stable and unstable

* Tel.: +91 512 259 7377.
E-mail address: vshankar@iitk.ac.in.

0377-0257/$ – see front matter © 2004 Elsevier B.V. All rights reserved.
doi:10.1016/j.jnnfm.2004.11.001

Nomenclature

$c = c_r + ic_i$ complex wave-speed
G shear modulus of the solid
H non-dimensional thickness of the solid
k wavenumber
R dimensional total thickness of the two fluids
V dimensional velocity of the top plate
$W_\alpha = \tau_\alpha V/R$ Weissenberg number of fluid α
Greek letters
β non-dimensional thickness of fluid 2
$(1-\beta)$ non-dimensional thickness of fluid 1
η_w viscosity of the solid layer
$\eta_r = \eta_w/\mu_b$ ratio of solid to fluid B viscosity
$\Gamma = V\eta/(GR)$ non-dimensional elasticity parameter of solid
μ_a viscosity of fluid A
μ_b viscosity of fluid B
$\mu_r = \mu_a/\mu_b$ ratio of fluid viscosities
$\Sigma = \gamma^*/(\eta V)$ non-dimensional fluid–fluid interfacial tension
τ_α relaxation time of fluid α

processing conditions could help prevent unwanted interfacial instabilities. In this paper, we consider the stability of two-layer viscoelastic plane Couette flow past a deformable solid layer (see Fig. 1) in order to explore the possibility of using the deformable solid layer to suppress the interfacial instabilities. When a fluid flows past a soft solid, the dynamics of the fluid and the solid medium get coupled, and waves can propagate across the fluid–solid interface as the shear moduli of soft solids are typically in the range 10^4–10^6 Pa [13–15]. When we consider two-layer flow past a deformable solid layer, one might expect the interfacial waves at the fluid–fluid interface and the fluid–solid interface to get coupled. This coupling of the two different 'interfacial modes' could lead to enhancement or suppression of the two-fluid interfacial instability. Indeed, an earlier study by the author [16] had analyzed the configuration of two-layer viscoelastic plane Couette flow past a deformable solid layer for the special case of matched fluid viscosities, and showed that it is possible (under appropriate conditions) to suppress the two-fluid interfacial instability due to elasticity stratification [1,2] by making the solid layer more deformable. The present study extends the previous results to the more general and experimentally relevant case of fluids with different viscosities. It is shown here that the presence of viscosity mismatch between the fluids has profound consequences on the stabilizing or destabilizing effect of the solid layer on the two-fluid interfacial mode due to elasticity stratification. In the rest of this Section, we recapitulate relevant previous literature on this subject, and motivate the context for the present study.

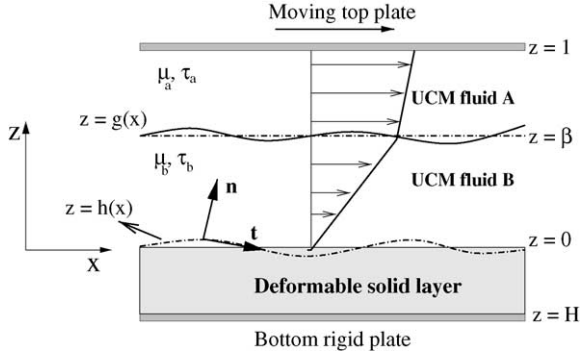

Fig. 1. Schematic diagram showing the configuration and (non-dimensional) coordinate system considered in Section 2: Two UCM fluids with viscosities μ_a and μ_b, and with relaxation times τ_a and τ_b flowing past a deformable solid layer.

The instability of the interface between two-layer plane Couette flow of upper convected Maxwell (abbreviated UCM henceforth) fluids was first predicted by Renardy [1] and Chen [2], respectively, in the short wave and long wave limits. These authors showed that if the relaxation times of the two fluids are different, then the discontinuity in the first normal stress difference between the two fluids drives an interfacial instability, which could happen even in the creeping flow limit (i.e. zero Reynolds number) and in the absence of viscosity difference between the two fluids. This is very different from the behaviour of two-layer plane Couette flow of Newtonian fluids, which becomes unstable only in the presence of fluid inertia (i.e. non-zero Reynolds number) and with viscosity difference between the two fluids. This was first predicted for two-layer Newtonian Couette flow by Yih [17] using a long wave asymptotic analysis. Subsequent studies [3,4,9–12] on the stability of two-layer and three-layer flows of viscoelastic fluids have considered both plane Couette and plane Poiseuille flows of UCM and Oldroyd-B fluids using asymptotic analyses and pseudospectral numerical methods. These studies have clearly identified the parameter regimes in which interfacial instabilities occur, and have explained the physical mechanisms that underlie these instabilities. For the special case of matched fluid viscosities, these studies show that when the thickness of the more elastic fluid is smaller (larger) than that of the less elastic fluid, the interface is unstable (stable) to long wavelength perturbations. Wilson and Khomami [5–8] have carried out a series of experimental studies on the interfacial instabilities in multilayer flows of viscoelastic fluids. Ganpule and Khomami [11] provide an extensive summary of the theoretical studies in this area. In this work, we refer to this instability due to elasticity stratification as the 'two-fluid interfacial mode' in the ensuing discussion.

Shankar and Kumar [14] studied the stability of a *single* layer UCM plane Couette flow past a deformable solid layer (modeled as a linear viscoelastic solid fixed to a rigid substrate) in the creeping flow limit. They showed that the interface between the UCM fluid and the solid becomes unstable when the solid layer becomes sufficiently deformable, i.e. when the non-dimensional parameter $\Gamma = V\mu(GR)$ ex-

ceeds a certain critical value, and when the non-dimensional group $\tau G/\mu$ (a modified Weissenberg number) is less than a certain critical value. Here, G is the shear modulus of the solid layer, μ the viscosity of the UCM fluid, V the velocity of the top plate driving the Couette flow, τ the relaxation time of the UCM fluid, and R is the thickness of the UCM fluid. The mechanism that drives this instability is the discontinuity of the base state velocity gradient at the fluid–solid interface, which couples the mean flow and the interfacial fluctuations even in the creeping flow limit via the tangential velocity condition at the fluid–solid interface. We refer to this instability as the 'fluid – solid interfacial mode' in the following discussion. This instability is qualitatively different from the interfacial instability between the two UCM fluids, which is driven by the discontinuity in the first normal stress difference at the fluid–fluid interface.

A recent study by the author [16] considered the stability of two-layer flow of UCM fluids with *matched viscosities*, but with different relaxation times, past a deformable solid layer in the creeping flow limit. The assumptions of matched viscosities and creeping flow allowed for an analytical treatment of the problem using the Gorodtsov–Leonov [18] eigenfunctions at arbitrary wavenumbers. The results of that study showed that when the more (less) elastic fluid is present in between the less (more) elastic fluid and the solid layer, the deformability of the solid layer has a stabilizing (destabilizing) effect on the two-fluid interfacial mode. It was shown that the non-dimensional solid elasticity parameter (defined above) $\Gamma \propto k^{-1}$ in the limit of $k \ll 1$ (k is the non-dimensional wavenumber of perturbations) in order to suppress the two-fluid interfacial mode. For $k \gg 1$, the solid layer does not have any effect on the two-fluid interfacial mode, and these short waves are stabilized by the non-zero interfacial tension between the two fluids. In general, increasing the solid layer deformability (i.e. Γ) further can destabilize the fluid–solid interfacial mode [14]. However, by carefully tuning the solid layer thickness H, shear modulus Γ, and the fluid–solid viscosity ratio η_r, it was shown that both the interfacial modes can be suppressed in finite experimental geometries. A similar study was carried out recently by Shankar and Kumar [19] for the case of two-layer flow of Newtonian fluids past a deformable solid layer.

However, the previous study was restricted to the special case of UCM fluids with matched viscosities, and to the creeping flow regime, where the inertial effects in the two fluids and the solid layer were neglected. In general situations of experimental interest in polymer processing applications, there is bound to be viscosity contrast between the two fluids, and the flow will occur at small (but finite) Reynolds number. Under such circumstances, there exists the possibility of an instability of the two-fluid interface due to viscosity stratification (similar to Yih's [17] instability for Newtonian fluids) apart from the instability due to elasticity stratification. Consequently, for UCM fluids with both viscosity and elasticity stratification, it is necessary to determine the effect of the deformable solid layer on combined viscosity and elasticity stratification in order to make connections with experimentally realistic situations.

The objective of the present work, therefore, is to study the stability of two-layer plane Couette flow of UCM fluids with different viscosities and relaxation times past a deformable solid layer at non-zero Reynolds number. We use the UCM model to represent the two viscoelastic fluids, as this model retains the essential physics to capture the purely elastic interfacial instability between the viscoelastic fluids. Owing to the general case considered here (finite Reynolds number and unequal viscosities), it is not possible to obtain analytical solutions to the stability problem for perturbations with arbitrary wavelengths. We, therefore, first carry out an asymptotic analysis in the low wavenumber limit (similar to the low wavenumber analysis of Chen [2]) to determine the effect of the deformable solid layer on the two-fluid interfacial mode. We then employ a numerical method to extend these low wavenumber results to finite values of wavenumber.

The rest of this paper is structured as follows: the relevant governing equations and boundary conditions are presented in Section 2.1, while the linearized stability equations are presented in Section 2.3. Section 3 outlines the low wavenumber asymptotic analysis, and highlights the important results from this analysis. We briefly describe the numerical method used to solve the equations governing the three-layer configuration in Section 4.1. Representative numerical results for the complex wavespeed as a function of wavenumber, as well as neutral stability curves in appropriate parameter space are presented in Section 4.2. Finally, Section 5 summarizes the important conclusions from the present study.

2. Problem formulation

2.1. Governing equations

The system under consideration (see Fig. 1) consists of a linear viscoelastic solid of thickness HR, shear modulus G, and viscosity η_w fixed onto a rigid surface at $z^* = -HR$, a layer of viscoelastic fluid (fluid B) of thickness βR in the region $0 < z^* < \beta R$ with viscosity μ_b, relaxation time τ_b, and another viscoelastic fluid layer (fluid A) of thickness $(1-\beta)R$ in the region $\beta R < z^* < R$ with viscosity μ_a, relaxation time τ_a. The two viscoelastic fluids are modeled using the UCM model (see, for example, [20]), which has two material constants: a constant viscosity μ and a constant relaxation time τ. We have assumed that the densities of the two fluids are equal ($\rho_a = \rho_b = \rho$), in order to exclusively focus on the instability of the two-fluid interface due to elasticity and viscosity stratification. In what follows, we indicate dimensional variables with a superscript $*$, and non-dimensional variables without any superscript. Fluid A is bounded at $z^* = R$ by a rigid wall, which moves at a constant velocity V in the x-direction relative to the deformable solid layer. The following scales are used for non-dimensionalising various physical quantities at the outset: R for lengths and displacements, V for

velocities, R/V for time, and $\mu_b V/R$ for stresses and pressure. H, therefore, is the non-dimensional thickness of the solid layer, while $(1-\beta)$ and β are, respectively, the non-dimensional thickness of fluids A and B.

The non-dimensional equations governing the dynamics of the two fluids are, respectively, the continuity and momentum conservation equations:

$$\partial_i v_i^\alpha = 0, \qquad \partial_j T_{ij}^\alpha = Re[\partial_t + v_j^\alpha \partial_j] v_i^\alpha. \tag{1}$$

Here, v_i^α is the velocity field in fluid α (α = a,b) and T_{ij}^α is the total stress tensor in fluid α, which is a sum of an isotropic pressure $-p^\alpha \delta_{ij}$ and the extra-stress tensor τ_{ij}^α:

$$T_{ij}^\alpha = -p^\alpha \delta_{ij} + \tau_{ij}^\alpha, \tag{2}$$

and the indices i, j take the values x, z. The extra-stress tensor is prescribed by the UCM constitutive relation as:

$$W_\alpha[\partial_t \tau_{ij}^\alpha + v_k^\alpha \partial_k \tau_{ij}^\alpha - \partial_k v_i^\alpha \tau_{kj}^\alpha - \partial_k v_j^\alpha \tau_{ki}^\alpha] + \tau_{ij}^\alpha = \mu_r^\alpha (\partial_i v_j^\alpha + \partial_j v_i^\alpha), \tag{3}$$

where $\partial_t \equiv (\partial/\partial t)$, $\partial_i \equiv (\partial/\partial x_i)$, $W_\alpha = \tau_\alpha V/R$ is the Weissenberg number in fluid α, and $Re = \rho V R/\mu_b$ is the Reynolds number based on the viscosity of fluid B. The quantity μ_r^α is the viscosity ratio in the two fluids, and this is defined such that $\mu_r^a \equiv \mu_r = \mu_a/\mu_b$, $\mu_r^b = \mu_b/\mu_b = 1$. No-slip boundary conditions are appropriate for fluid A at $z = 1$:

$$v_x^a = 1, \qquad v_z^a = 0, \tag{4}$$

while the boundary conditions at the interface between the two UCM fluids and the interface between the fluid and the solid layer are discussed below.

The deformable solid layer is modeled as an incompressible linear viscoelastic solid, similar to that used in the previous studies in this area (see, for example, [14,13,21,22]). The dynamics of the solid layer is described by a displacement field u_i, which represents the displacement of the material points in the medium from their steady-state positions. The velocity field in the solid layer is $v_i = \partial_t u_i$. In an incompressible linear viscoelastic solid, the displacement field satisfies the continuity equation:

$$\partial_i u_i = 0. \tag{5}$$

The momentum conservation equation in the solid is given by:

$$\partial_j \Pi_{ij} = Re \partial_t^2 u_i, \tag{6}$$

where $\Pi_{ij} = -p_g \delta_{ij} + \sigma_{ij}$ is the total stress tensor, which is given by a sum of the isotropic pressure p_g and deviatoric stress σ_{ij}. Without loss of generality, it is assumed here that the density of the solid is equal to the density of the two fluids. The deviatoric stress tensor σ_{ij} is given by a sum of elastic and viscous stresses in the solid layer:

$$\sigma_{ij} = \left(\frac{1}{\Gamma} + \eta_r \partial_t\right)(\partial_i u_j + \partial_j u_i), \tag{7}$$

where $\Gamma = V\mu_b/(GR)$ is the non-dimensional quantity characterizing the elasticity of the solid layer and $\eta_r = \eta_w/\mu_b$ is the ratio of solid and fluid B viscosities. More precisely, $1/\Gamma$ is the estimated ratio of elastic stresses in the solid layer to viscous stresses in fluid B. The solid layer is assumed to be fixed to a rigid surface at $z = -H$, and the boundary condition for the displacement field there is $u_i = 0$. A recent study by Gkanis and Kumar [23] (also see [14]) on the stability of the plane Couette flow of a Newtonian fluid past a deformable solid has examined the role of non-linear rheological properties in the solid by modeling the deformable solid using the neo-Hookean model. In the present study, however, we restrict ourselves to the simple linear viscoelastic solid model because the numerical values of Γ required to realize the phenomena predicted in this study are shown to be typically much lower than unity, and consequently, it is argued later that the results from the linear solid model are expected to be accurate.

The conditions at the interface $z = g(x)$ between the two UCM fluids are the continuity of the velocities and stresses, and the kinematic condition for the evolution of the interfacial position $g(x)$. The conditions at the interface $z = h(x)$ between UCM fluid 2 and the solid layer are the continuity of the velocities and stresses. We neglect the effect of interfacial tension between UCM fluid B and the solid layer, as this was found [13] to have a purely stabilizing effect on the interfacial mode of the interface at $z = h(x)$ between the fluid and the solid layer.

2.2. Base state

The steady velocity profiles are simply the Couette flow velocity profiles in the two fluids, with different gradients due to the difference in viscosities of the two fluids:

$$\bar{v}_x^a = \frac{z + \beta(\mu_r - 1)}{1 + \beta(\mu_r - 1)}, \qquad \bar{v}_z^a = 0, \tag{8}$$

$$\bar{\tau}_{xx}^a = 2W_a \frac{\mu_r}{[1 + \beta(\mu_r - 1)]^2}, \qquad \bar{\tau}_{zz}^a = 0,$$
$$\bar{\tau}_{xz}^a = \bar{\tau}_{zx}^a = \frac{\mu_r}{1 + \beta(\mu_r - 1)}, \tag{9}$$

$$\bar{v}_x^b = \frac{\mu_r z}{1 + \beta(\mu_r - 1)}, \qquad \bar{v}_z^b = 0, \tag{10}$$

$$\bar{\tau}_{xx}^b = 2W_b \frac{{\mu_r}^2}{[1 + \beta(\mu_r - 1)]^2}, \qquad \bar{\tau}_{zz}^b = 0,$$
$$\bar{\tau}_{xz}^b = \bar{\tau}_{zx}^b = \frac{\mu_r}{1 + \beta(\mu_r - 1)}, \tag{11}$$

Note that the non-zero first normal stress difference $\bar{\tau}_{xx}^{(\alpha)} - \bar{\tau}_{zz}^{(\alpha)}$ (α = a, b) is different in the two fluids, and it is discontinuous across the two-fluid interface. The solid layer is at rest in this steady base state, but there is a non-zero unidirectional displacement $\bar{u}_x$ due to the fluid shear stresses at the

interface:

$$\bar{u}_x = \frac{\Gamma\mu_r(z+H)}{1+\beta(\mu_r-1)}, \qquad \bar{u}_z = 0,$$
$$\bar{\sigma}_{xx} = 0, \qquad \bar{\sigma}_{zz} = 0, \tag{12}$$

$$\bar{\sigma}_{xz} = \bar{\sigma}_{zx} = \frac{\mu_r}{1+\beta(\mu_r-1)}. \tag{13}$$

All the base flow quantities above are denoted with an overbar in the preceding and ensuing discussions.

2.3. Linear stability analysis

We use a temporal stability analysis to determine the fate of small perturbations to the above base state. Small perturbations (primed quantities) are introduced to all dynamical quantities about their base state values, e.g., $v_i^\alpha = \bar{v}_i^\alpha + v_i^{\alpha'}$. The perturbation quantities are expanded in terms of Fourier modes in the x-direction, and with an exponential time dependence: $v_i^{\alpha'} = \tilde{v}_i^{\alpha'}(z)\exp[ik(x-ct)]$. Here, k is the wavenumber, c the wavespeed, and $\tilde{v}_i^\alpha(z)$ are eigenfunctions which are determined below from the linearized governing equations and boundary conditions. The complex wavespeed $c = c_r + ic_i$, and when $c_i > 0$, the base state is temporally unstable.

Upon substituting the above form for the perturbations in the governing equations for the two fluids (1) and the constitutive relation for the two UCM fluids (3), we obtain the following linearized equations for the two fluids, where α = a,b and $\mathrm{d}_z = \mathrm{d}/\mathrm{d}z$:

$$\mathrm{d}_z\tilde{v}_z^\alpha + ik\tilde{v}_x^\alpha = 0, \tag{14}$$
$$-ik\tilde{p}^\alpha + ik\tilde{\tau}_{xx}^\alpha + \mathrm{d}_z\tilde{\tau}_{xz}^\alpha = Re[ik(\bar{v}_x^\alpha - c)\tilde{v}_x^\alpha + \mathrm{d}_z\bar{v}_x^\alpha\tilde{v}_z^\alpha], \tag{15}$$
$$-\mathrm{d}_z\tilde{p}^\alpha + \mathrm{d}_z\tilde{\tau}_{zz}^\alpha + ik\tilde{\tau}_{xz}^\alpha = Re[ik(\bar{v}_x^\alpha - c)]\tilde{v}_z^\alpha, \tag{16}$$
$$\{1 + ikW_\alpha(\bar{v}_x^\alpha - c)\}\tilde{\tau}_{zz}^\alpha = 2\mu_r^\alpha\mathrm{d}_z\tilde{v}_z^\alpha + 2ikW_\alpha\bar{\tau}_{xz}^\alpha\tilde{v}_z^\alpha, \tag{17}$$
$$\{1 + ikW_\alpha(\bar{v}_x^\alpha - c)\}\tilde{\tau}_{xz}^\alpha = \mu_r^\alpha(\mathrm{d}_z\tilde{v}_x^\alpha + ik\tilde{v}_z^\alpha) + W_\alpha(\mathrm{d}_z\bar{v}_x^\alpha\tilde{\tau}_{zz}^\alpha + ik\bar{\tau}_{xx}^\alpha\tilde{v}_z^\alpha), \tag{18}$$
$$\{1 + ikW_\alpha(\bar{v}_x^\alpha - c)\}\tilde{\tau}_{xx}^\alpha = 2\mu_r^\alpha ik\tilde{v}_x^\alpha + 2W_\alpha(\mathrm{d}_z\bar{v}_x^\alpha\tilde{\tau}_{xz}^\alpha + ik\bar{\tau}_{xx}^\alpha\tilde{v}_x^\alpha + \bar{\tau}_{xz}^\alpha\mathrm{d}_z\tilde{v}_x^\alpha). \tag{19}$$

It is possible to derive a single fourth order differential equation governing $\tilde{v}_z^\alpha$ from the above set of equations, similar to Gorodtsov and Leonov [18] for the case of a single layer UCM plane Couette flow. However, owing to the prefactors in the base-flow velocity profiles and stresses in the two-layer case (unlike in the single layer problem), the equation is quite cumbersome. For this reason, the explicit form of the fourth order differential equation is not displayed here.

The governing equations for the displacement field in the solid layer can be expressed in terms of $\tilde{u}_i(z)$ in a similar manner to give:

$$\mathrm{d}_z\tilde{u}_z + ik\tilde{u}_x = 0, \tag{20}$$
$$-ik\tilde{p}_g + \left(\frac{1}{\Gamma} - ikc\eta_r\right)(\mathrm{d}_z^2 - k^2)\tilde{u}_x = -Rek^2c^2\tilde{u}_x, \tag{21}$$
$$-\mathrm{d}_z\tilde{p}_g + \left(\frac{1}{\Gamma} - ikc\eta_r\right)(\mathrm{d}_z^2 - k^2)\tilde{u}_z = -Rek^2c^2\tilde{u}_z. \tag{22}$$

These equations can be reduced to a single fourth-order differential equation for $\tilde{u}_z$:

$$(1 - ikc\eta_r\Gamma)(\mathrm{d}_z^2 - k^2)^2\tilde{u}_z + Rek^2c^2\Gamma(\mathrm{d}_z^2 - k^2)\tilde{u}_z = 0. \tag{23}$$

The linearized boundary conditions at the unperturbed interface position $z = 0$, between UCM fluid B and the solid layer are given by [16,14]:

$$\tilde{v}_z^b = (-ikc)\tilde{u}_z, \tag{24}$$
$$\tilde{v}_x^b + [\mathrm{d}_z\bar{v}_x^b]_{z=0}\tilde{u}_z = (-ikc)\tilde{u}_x, \tag{25}$$
$$-\tilde{p}^b + \tilde{\tau}_{zz}^b = -\tilde{p}_g + 2\left(\frac{1}{\Gamma} - ikc\eta_r\right)\mathrm{d}_z\tilde{u}_z, \tag{26}$$
$$\tilde{\tau}_{xz}^b - ik\bar{\tau}_{xx}^b\tilde{u}_z = \left(\frac{1}{\Gamma} - ikc\eta_r\right)(\mathrm{d}_z\tilde{u}_x + ik\tilde{u}_z). \tag{27}$$

Here, the second term in the left side of Eqs. (25) and (27) represent non-trivial contributions that arise as a result of the Taylor expansion of the mean flow quantities about the unperturbed fluid–solid interface. The additional term that appears in Eq. (25) for the tangential velocity is responsible for the instability of the interface between the fluid and the deformable solid layer [13,14].

Similarly, the linearized boundary conditions at the unperturbed interface position $z = \beta$ between the two UCM fluids A and B are given by:

$$\tilde{v}_z^a = \tilde{v}_z^b, \tag{28}$$
$$\tilde{v}_x^a + [\mathrm{d}_z\bar{v}_x^a]_{z=\beta}\tilde{g} = \tilde{v}_x^b + [\mathrm{d}_z\bar{v}_x^b]_{z=\beta}\tilde{g}, \tag{29}$$
$$-\tilde{p}^a + \tilde{\tau}_{zz}^a - \Sigma k^2\tilde{g} = -\tilde{p}^b + \tilde{\tau}_{zz}^b \tag{30}$$
$$\tilde{\tau}_{xz}^a - ik\bar{\tau}_{xx}^a\tilde{g} = \tilde{\tau}_{xz}^b - ik\bar{\tau}_{xx}^b\tilde{g}, \tag{31}$$

where $\tilde{g}$ is the Fourier expansion coefficient for the interface position $g = \tilde{g}\exp[ik(x-ct)]$, and $\Sigma = \gamma^*/(\mu_b V)$ is the non-dimensional interfacial tension between UCM fluids A and B. Note that in the tangential velocity condition (Eq. (29)), there are additional terms that arise due to Taylor expansion because of the discontinuity in the velocity gradient at $z = \beta$ in the base state. The tangential stress condition (Eq. (31)) has additional terms due to the jump in the first normal stress difference across the two-fluid interface in the base state. These additional terms are responsible for the purely elastic interfacial instability in two-layer flows of UCM fluids. The linearized kinematic condition at $z = \beta$ between the

two UCM fluids is given by:

$$ik[\overline{v_x^a}(z=\beta)-c]\tilde{g}=\tilde{v}_z^a[z=\beta]. \tag{32}$$

The boundary conditions at $z=1$ are simply:

$$\tilde{v}_z^a=0, \qquad \tilde{v}_x^a=0, \tag{33}$$

while the boundary conditions at $z=-H$ are:

$$\tilde{u}_z=0, \qquad \tilde{u}_x=0. \tag{34}$$

Differential Eqs. (14)–(19) for the two fluids and (20)–(22) for the solid layer along with interface and boundary conditions (24)–(34) completely specify the stability problem for the three-layer configuration of interest in this study. The complex wavespeed c is a function of Re, W_α, Γ, k, H, β, Σ, η_r and μ_r. For arbitrary Re, k, and μ_r, there are no closed form solutions to the governing fluid stability equations, and so a numerical method must be used to solve the stability problem in general. However, when we consider very long waves, i.e. $k \ll 1$, an asymptotic analysis in the small parameter k is possible, similar to the analysis of Chen [2] for two-layer Couette flow of UCM fluids, which yields an analytical expression for the wavespeed as an asymptotic series in k. In the next section, we briefly outline the low wavenumber asymptotic analysis and the results obtained from that analysis. These low-k results are then used as starting guesses for a complete numerical treatment of the stability problem in Section 4.2.

3. Low wavenumber asymptotic analysis

In this section, the effect of a third solid layer on the stability of the two-layer UCM plane Couette flow is analyzed in the limit $k \ll 1$, with $Re \sim O(1)$ and $\Gamma \sim O(1)$. For $k \ll 1$, the complex wavespeed c is expanded in an asymptotic series in k:

$$c=c^{(0)}+kc^{(1)}+\cdots. \tag{35}$$

The low wavenumber asymptotic analysis for the present three-layer configuration is very similar to the analyses of Yih [17] and Chen [2], respectively, for two-layer flows of Newtonian and UCM fluids in rigid channels, and to the analysis of Shankar and Kumar [19] for two-layer flow of Newtonian fluids past a deformable solid layer. Therefore, in the interests of brevity, we do not present the details of the calculation. Briefly, the velocities and stresses in the two fluids are expanded to $O(k)$, and only the leading order displacement field in the solid is required in the low-k analysis. The differential equations governing the leading order and first correction to the fluid velocity fields, and the leading order displacement field in the solid are solved analytically. The governing differential equations in the two fluids are of order four, so the solutions in each fluid contain four constants to be fixed by the interface and boundary conditions. The solution to the displacement field in the solid also has four constants, but two of them are eliminated after using the boundary conditions at $y=-H$. The leading order and first correction solutions to the velocity, pressure, stress fields in the two fluid layers, solution to the leading order displacement and pressure fields in the solid layer are inserted in the asymptotic expansions for the various dynamical quantities, which are then substituted in the boundary and interface conditions (Eqs. (24)–(33)). These are expressed in the following matrix form:

$$\mathbf{M}\cdot\mathbf{C}^{\mathrm{T}}=0, \tag{36}$$

where $\mathbf{C}$ is the vector of coefficients and $\mathbf{M}$ is a 10×10 matrix, whose rows represent the different interface and boundary conditions. The characteristic equation is obtained by setting the determinant of the matrix $\mathbf{M}$ to zero. In the low wavenumber asymptotic analysis, the determinant of this matrix is expanded in a series in k, as follows:

$$f_0(c^{(0)})+kf_1(c^{(0)},c^{(1)})+\cdots=0, \tag{37}$$

where f_0 is the leading order term in the determinant, and f_1 is the first correction. The leading order, first correction and higher order terms must be separately zero for the determinant to be zero, i.e.,

$$f_0(c^{(0)})=0, \quad f_1(c^{(0)},c^{(1)})=0,\ldots. \tag{38}$$

These algebraic equations can then be sequentially solved to obtain expressions for $c^{(0)}$ and $c^{(1)}$. The above procedure was implemented using the symbolic package *Mathematica*. In the low wavenumber limit, the wavespeed c in the present problem is a function of Re, Γ, W_a, W_b, μ_r, η_r, H, β, and Σ. The parameter $\Gamma=V\mu_b/(GR)$ is the ratio of viscous stresses in fluid B to elastic stresses in the solid layer, and when $\Gamma\to 0$, we obtain the rigid solid limit. We have validated the procedure of our asymptotic analysis by comparing our asymptotic results with the results of Yih [17] for the case of two-layer plane Couette flow of Newtonian fluids in a rigid channel ($W_a=0$, $W_b=0$, and $\Gamma=0$), and also by comparing our asymptotic results with the results of Chen [2] for the case of two-layer plane Couette flow of UCM fluids in a rigid channel ($\Gamma=0$).

For the three-layer configuration of interest in this study, our asymptotic analysis shows that at leading order, $c^{(0)}$ is purely real, and is identical to Yih's [17] result for leading order wavespeed in the two-layer plane Couette flow of *Newtonian* fluids in a rigid channel. In other words, the normal stress differences between the two viscoelastic fluids and the effect of soft solid layer do not appear at the leading order problem in the present three layer configuration. Thus, in order to determine the stability of the system, one must calculate the first correction $c^{(1)}$. Our asymptotic analysis shows that in the $k\to 0$ limit, the parameters Σ (interfacial tension) and η_r (solid to fluid viscosity ratio) do not appear in $c^{(0)}$ and $c^{(1)}$. The analytical expression for $c^{(1)}$ is very complicated when the remaining parameters Re, W_a, W_b, Γ, μ_r, H, and β are left unspecified. However, when only β and μ_r are specified,

it is possible to obtain analytical expressions for $c^{(1)}$ with the other parameters being left unspecified.

An illustration of the present asymptotic result to $O(k)$ for $\beta = 0.4$ and $\mu_r = 0.5$ is given here:

$$c = c^{(0)} + kc^{(1)}, \tag{39}$$

$$c^{(0)} = 0.31447, \tag{40}$$

$$c^{(1)} = \mathrm{i}[0.018(W_b - 1.13W_a) + 0.00012\,Re - 0.034\Gamma H(H^2 + 2.24H + 1.5)]. \tag{41}$$

The result for $c^{(0)}$ (which is a real quantity) is identical to that of Yih [17] for the case of two-layer plane Couette flow of Newtonian fluids in a rigid channel (without the deformable solid layer). The first correction $c^{(1)}$, however, is purely imaginary, and has three distinct contributions: the first term proportional to the difference between W_b and W_a is destabilizing when $W_b > 1.13W_a$, and it is identical to Chen's [2] result for the instability of two-layer plane Couette flow of UCM fluids in rigid channels due to elasticity stratification. The second term proportional to Re is also destabilizing, and is identical to that of Yih's [17] result for two-layer Newtonian plane Couette flow due to viscosity stratification. The third term on the right side of Eq. (41), which is proportional to the product ΓH represents the effect of the deformable solid layer on the two-fluid interfacial mode. This term due to the solid layer deformability has a negative sign and therefore is *stabilizing*. The solid elasticity parameter $\Gamma = V\mu_b/(GR)$ is the ratio of viscous stresses in fluid B to elastic stresses in the solid layer, and $\Gamma \to 0$ is the limit of a rigid solid layer. H is the non-dimensional thickness of the solid layer, and when $H = 0$, the fluid B flows past the bottom rigid wall at $y = -H$. As the shear modulus of the solid decreases, Γ increases, thus, making the solid more deformable. As might be expected, the effect of the solid layer on the two-fluid interfacial mode vanishes when $\Gamma = 0$ (limit of a rigid solid layer) and when $H = 0$ (limit of no solid layer). However, for finite Γ and H, the solid layer has a stabilizing effect on the two fluid interfacial instability. From the above expression for $c^{(1)}$, the parameter Γ required for neutrally stable modes can be obtained by setting $\mathrm{Im}[c^{(1)}] = 0$:

$$\Gamma_0 = \frac{0.0035\,Re + 0.529\,(W_b - 1.13\,W_a)}{H(H^2 + 2.24\,H + 1.5)}, \tag{42}$$

where the subscript '0' refers to the low wavenumber asymptotic result. We illustrate the above result for the specific case of $W_b = 2$ and $W_a = 1$:

$$\Gamma_0 = \frac{0.46(1 + 0.0076Re)}{H(H^2 + 2.24\,H + 1.5)}. \tag{43}$$

For $Re \sim O(1)$, the prefactor multiplying Re is very small compared to 1, and so the contribution due to viscosity stratification is negligible compared to the contribution from elasticity stratification in the numerator. For a specified solid layer thickness H, when the non-dimensional group Γ is greater than the value given by the above expression, the two-fluid interfacial instability is stabilized in the low wavenumber limit.

For $\mu_r = 0.5$, $\beta = 0.8$, the result from our asymptotic analysis is given by:

$$c^{(0)} = 0.720214, \tag{44}$$

$$c^{(1)} = \mathrm{i}[0.013(W_a - 1.148W_b) - 0.00016Re + 0.036\Gamma H(H^2 + H + 0.26)], \tag{45}$$

For this case too, $c^{(0)}$ is identical to Yih's result for two-layer Newtonian plane Couette flow and $c^{(1)}$ has three distinct contributions. The first term in the expression for $c^{(1)}$ proportional to the difference between W_a and W_b is negative if $W_a < 1.148W_b$, and the second term proportional to Re is also negative. The third term representing the effect of the solid layer on the two-fluid interfacial mode, however, is positive, and is *destabilizing* for all values of H. This illustration shows that the solid layer could also have a destabilizing effect on the two-fluid interfacial mode, while it is stable when $W_a < 1.148W_b$ in the absence of the solid layer.

In general, our asymptotic result for c can, thus, be represented as:

$$c = c^{(0)} + k(c^{(1)}_{\mathrm{elas}} + c^{(1)}_{\mathrm{visc}} + c^{(1)}_{\mathrm{solid}}). \tag{46}$$

Here, $c^{(0)}$ is purely real, and is identical to the leading order wavespeed obtained for two-layer plane Couette flow of Newtonian fluids by Yih [17]. All the three distinct contributions to $c^{(1)}$ are purely imaginary quantities, and each could have a stabilizing or destabilizing effect on the two-fluid interfacial mode. Firstly, $c^{(1)}_{\mathrm{elas}}$ is the contribution due to elasticity stratification between the two fluids and is proportional to the difference in W_a and W_b, and this is identical to the long-wave result of Chen [2] for two-layer flow of viscoelastic (UCM) fluids. Secondly, $c^{(1)}_{\mathrm{visc}}$ is the contribution due to viscosity stratification between the two fluids and is proportional to Re, and this is identical to the result of Yih [17] for two-layer flow of Newtonian fluids. Finally, $c^{(1)}_{\mathrm{solid}}$ is the effect of the solid layer deformability on the two-fluid interfacial mode, which is the contribution from the present asymptotic analysis.

Tables 1 and 2 summarize the results for the three distinct contributions to $c^{(1)}$ obtained from the low wavenumber analysis for two different thickness ratios $\beta = 0.4$ and $\beta = 0.6$ for various values of μ_r. Let us first focus on Table 1. This table shows that, for $\beta = 0.4$, the solid layer has a stabilizing effect on the two-fluid interfacial mode when $\mu_r < 1$, and it has a destabilizing effect when $\mu_r > 1$. Interestingly, we find that for $|\mu_r - 1| \ll 1$, $c^{(1)}_{\mathrm{solid}} \propto (\mu_r - 1)$, and when $\mu_r = 1$, $c^{(1)}_{\mathrm{solid}} = 0$, i.e. the solid layer has no effect on the two-fluid interfacial mode when the viscosities of the two fluids are the same. Similarly, we find that the contribution due to viscosity stratification $c^{(1)}_{\mathrm{visc}} \propto (1 - \mu_r)$, and it vanishes for $\mu_r = 1$. Importantly, the results presented in these tables indicate that the stabilizing or destabilizing nature of the solid layer on the

Table 1
Summary of results from low wavenumber analysis for $\beta = 0.4$ and $\Gamma \sim O(1)$

μ_r	$\mathrm{Im}[c^{(1)}_{elas}]$	$\mathrm{Im}[c^{(1)}_{visc}]$	$\mathrm{Im}[c^{(1)}_{solid}]$
0.2	$0.012(W_b - 1.75W_a)$	$7.37 \times 10^{-4} Re$	$-0.048\Gamma H(H^2 + 2.08H + 1.36)$
0.4	$0.018(W_b - 1.21W_a)$	$1.98 \times 10^{-4} Re$	$-0.042\Gamma H(H^2 + 2.18H + 1.44)$
0.6	$0.0174(W_b - 1.07W_a)$	$7.49 \times 10^{-5} Re$	$-0.026\Gamma H(H^2 + 2.32H + 1.57H)$
0.8	$0.0148(W_b - 1.017W_a)$	$2.59 \times 10^{-5} Re$	$-0.011\Gamma H(H^2 + 2.5H + 1.75)$
1	$0.01152(W_b - W_a)$	0	0
1.1	$0.0098(W_b - 1.005W_a)$	$-8.96 \times 10^{-6} Re$	$4.13 \times 10^{-3}\Gamma H(H^2 + 2.9H + 2.16)$
2	$0.0008(W_a - 3.94W_b)$	$-4.8 \times 10^{-5} Re$	$0.007\Gamma H(H + 1.03)(H + 8.92)$
4	$0.008(W_a - 2.1W_b)$	$-7.06 \times 10^{-5} Re$	$-0.0963\Gamma H(H - 1.22)(H + 0.87)$
6	$0.0086(W_a - 2.73W_b)$	$-7.2 \times 10^{-5} Re$	$-0.247\Gamma H(H - 0.48)(H + 0.8)$

two-fluid interfacial mode is controlled only by the viscosity ratio between the two fluids, and is independent of the relaxation times (i.e. W_a and W_b). In a similar manner, Table 2 shows for $\beta = 0.6$ that the solid layer has a stabilizing effect on the two-fluid interfacial mode when $\mu_r > 1$, and could be stabilizing or destabilizing (depending on H and β) when $\mu_r < 1$. Here too, we find that the contribution to $c^{(1)}$ due to the solid layer $c^{(1)}_{solid} \propto (1 - \mu_r)$ for $|\mu_r - 1| \ll 1$, and it vanishes when $\mu_r = 1$.

It is appropriate at this point to compare and contrast the present asymptotic results with the previous analytical results of Shankar [16], who studied the effect of the solid layer deformability on the two-fluid interfacial instability with elasticity stratification, for the special case when $\mu_r = 1$. In that study, the author had used the exact solutions (for arbitrary k; first used by Gorodtsov and Leonov [18]) to the linear stability problem in the creeping flow limit for the two fluids, and the results of the stability analysis showed that the non-dimensional parameter $\Gamma \propto k^{-1}$ for $k \ll 1$ in order for the solid layer to have an effect on the two fluid interfacial mode with matched viscosities. Our asymptotic results discussed above showed that the effect of the solid layer on the two-fluid interfacial mode ($c^{(1)}_{solid} \propto |\mu_r - 1|$) vanishes for $\mu_r = 1$. There is, however, no inconsistency between the present asymptotic results for $\mu_r = 1$ and the previous results since in our asymptotic analysis we have stipulated at the outset that the non-dimensional solid elasticity parameter $\Gamma \sim O(1)$ (meaning it does not scale with k for $k \ll 1$). When $\mu_r \neq 1$, this assumption turns out to be sufficient in order for the solid layer to have an effect on the two-fluid interfacial mode. However, when $\mu_r = 1$, our asymptotic result shows that $c^{(1)}_{solid} = 0$, and this implies that $\Gamma \sim O(1)$ is not sufficient for the solid layer to have an effect. It is useful to recall that $\Gamma \to 0$ represents the rigid solid layer limit, and when Γ increases, the solid layer becomes more deformable. Physically, we expect the solid layer to be deformable in order for the interfacial fluctuations at the fluid B–solid interface to have an effect on the fluid–fluid interface. What the asymptotic results reveal is that when $\mu_r \neq 1$, it is sufficient to have $\Gamma \sim O(1)$, whereas for $\mu_r = 1$, we require $\Gamma \sim O(1/k) \gg 1$ which physically corresponds to a very soft solid layer. We have further verified that in the present asymptotic analysis, when $\mu_r = 1$, if we let $\Gamma \propto k^{-1}$, our asymptotic results agree with the earlier results of Shankar [16] obtained for the special case of matched fluid viscosities. This discussion, therefore, illustrates the importance of viscosity contrast between the two fluids in the effect of the solid layer on the two-fluid interfacial mode.

Another crucial difference between the present results for $\mu_r \neq 1$ and the previous results [16] obtained for matched viscosities is the role of viscosity contrast between the two fluids on the stabilizing or destabilizing nature of the solid layer. When μ_r is exactly equal to 1, the previous results [16] show that when the more (less) elastic fluid is present in between the less (more) elastic fluid and the solid layer, then the solid layer has a stabilizing (destabilizing) effect. However, the results presented in Tables 1 and 2 for $\mu_r \neq 1$ demonstrate that the stabilizing or destabilizing nature of the solid layer ($c^{(1)}_{solid}$) is controlled only by the viscosity ratio, and is independent of W_a and W_b. Indeed, for fixed values of W_a and W_b, the effect of the solid layer turns from stabilizing to destabilizing as μ_r crosses 1. Moreover, even minor viscos-

Table 2
Summary of results from low wavenumber analysis for $\beta = 0.6$ and $\Gamma \sim O(1)$

μ_r	$\mathrm{Im}[c^{(1)}_{elas}]$	$\mathrm{Im}[c^{(1)}_{visc}]$	$\mathrm{Im}[c^{(1)}_{solid}]$
0.2	$0.0088(W_b - 2.37W_a)$	$-3.64 \times 10^{-4} Re$	$-0.034\Gamma H(H^2 + 2.89H + 2.18)$
0.4	$0.0041(W_b - 2.018W_a)$	$-8.37 \times 10^{-3} Re$	$-0.0037\Gamma H(H + 10.02)(H + 1.03)$
0.6	$0.00093(W_a - 2.43W_b)$	$-6.4 \times 10^{-5} Re$	$0.007\Gamma H(H - 2.74)(H + 0.93)$
0.8	$0.00727(W_a - 1.035W_b)$	$-2.43 \times 10^{-5} Re$	$0.0069\Gamma H(H - 1.08)(H + 0.88)$
1	$0.01152(W_a - W_b)$	0	0
1.1	$0.013(W_a - 1.00357W_b)$	$9.21 \times 10^{-6} Re$	$-5.04 \times 10^{-3}\Gamma H(H - 0.456)(H + 0.828)$
2	$0.018(W_a - 1.13W_b)$	$6 \times 10^{-5} Re$	$-0.0685\Gamma H(H + 0.019)(H + 0.738)$
4	$0.014(W_a - 1.52W_b)$	$1.2 \times 10^{-4} Re$	$-0.1967\Gamma H(H + 0.267)(H + 0.629)$
6	$0.0098(W_a - 2W_b)$	$1.65 \times 10^{-4} Re$	$-0.271\Gamma H(H + 0.378)(H + 0.548)$

Table 3
Summary of results from low wavenumber analysis for $\mu_r = 0.5$ and $\Gamma \sim O(1)$

β	$\mathrm{Im}[c^{(1)}_{\mathrm{elas}}]$	$\mathrm{Im}[c^{(1)}_{\mathrm{visc}}]$	$\mathrm{Im}[c^{(1)}_{\mathrm{solid}}]$
0.2	$0.0099(W_b - 1.08W_a)$	$1.78 \times 10^{-4} Re$	$-0.019\Gamma H(H^2 + 1.88H + 1.14)$
0.4	$0.018(W_b - 1.13W_a)$	$1.2 \times 10^{-4} Re$	$-0.034\Gamma H(H^2 + 2.24H + 1.5)$
0.5	$0.011(W_b - 1.21W_a)$	$2.86 \times 10^{-6} Re$	$-0.02\Gamma H(H^2 + 3H + 2.26)$
0.6	$0.0008(W_b - 3.94W_a)$	$-9.6 \times 10^{-5} Re$	$0.003\Gamma H(H - 7.92)(H + 0.97)$
0.8	$0.0128(W_a - 1.48W_b)$	$-1.55 \times 10^{-4} Re$	$0.036\Gamma H(H^2 + H + 0.26)$

ity contrasts between the two fluids are sufficient to change the stabilizing/destabilizing nature of the solid layer. In the present analysis with $\mu_r \neq 1$, the difference in W_a and W_b is responsible only for the destabilization of the two-fluid interface (through the contribution $c^{(1)}_{\mathrm{elas}}$), and has no role on the effect of the solid layer on the two-fluid interfacial mode. In contrast, the previous results for matched fluid viscosities show that the stabilizing/destabilizing effect of the solid layer depends on the difference between W_a and W_b. Thus, the previous conclusions [16] obtained for matched fluid viscosities must be viewed as a special case insofar as the effect of the solid layer is concerned, and for general situations of experimental interest (where one will encounter viscosity contrasts) the conclusions of the present study are more relevant.

Tables 3 and 4 display the results obtained for two different viscosity ratios $\mu_r = 0.5, 2$ for various values of thickness ratio β. These tables show that for $\mu_r < 1$, $\beta < 0.5$ and $\mu_r > 1$, $\beta > 0.5$ the solid layer has a stabilizing effect, while for $\mu_r < 1$, $\beta > 0.5$ and $\mu_r > 1$, $\beta < 0.5$ the solid layer has both destabilizing and stabilizing effect (depending on H and β) on the two-fluid interfacial mode. Therefore, by appropriate combinations of W_a, W_b, β, and μ_r it is possible to stabilize (destabilize) the two-fluid interfacial mode due to elasticity and viscosity stratification by making the solid layer deformable, while it is unstable (stable) in the absence of the solid layer.

The above asymptotic results, however, are valid only in the limit of very long wave perturbations. In order to ascertain whether the predicted stabilization or destabilization of the two-fluid interfacial mode by the deformable solid layer extends to finite wavenumber perturbations, it is necessary to solve the governing stability equations for the present three layer configuration using a numerical method. In addition to the two-fluid interfacial mode, there exists an interfacial mode between fluid B and the deformable solid layer [14], and it was shown by Shankar and Kumar [14] that this interfacial mode becomes unstable to *finite* wavenumber perturbations when the solid elasticity parameter Γ exceeds a certain critical value. If we envisage the use of deformable solid layers to suppress the two-fluid interfacial instability, it is important that the fluid B–solid interfacial mode is not destabilized. Therefore, it is necessary to determine the regions in the Γ–k plane, where both the interfacial modes are stable. To this end, we briefly describe the numerical method used to solve the present three-layer stability problem in the following subsection and then discuss the results obtained from the numerical solution.

4. Results from numerical method

4.1. Numerical method

We use a numerical shooting procedure [24] to solve the fourth order ordinary differential equations in each layer. A fourth order Runge–Kutta integrator with adaptive step size control is used to obtain numerical representations of the linearly independent solutions to the fourth order differential equations. For fluid A, there are two linearly independent solutions consistent with the two boundary conditions at $z = 1$, and these are obtained by numerically integrating the fourth order stability equation from $z = 1$ to $z = \beta$. The velocity field $\tilde{v}^a_z$ in fluid A is then obtained as a linear combination of these two linearly independent solutions. For fluid B, which is bounded by fluid A and the solid layer on either side, we obtain four linearly independent solutions by numerically integrating from $z = \beta$ to $z = 0$. For the solid layer, we obtain two linearly independent solutions consistent with the boundary conditions at $z = -H$ by numerically integrating from $z = -H$ to $z = 0$. Thus, there are eight coefficients multiplying the linearly independent solutions (two in fluid A, four in fluid B, and two in the solid layer) in the three layers. The numerical solutions obtained in this manner are substituted in the eight interface conditions at $z = 0$ and $z = \beta$ (Eqs (24)–(31)) and a 8×8 characteristic matrix is obtained. The determinant of the characteristic matrix is set to zero to obtain the characteristic equation, which is solved using a Newton–Raphson iteration scheme to obtain the complex wavespeed.

Table 4
Summary of results from low wavenumber analysis for $\mu_r = 2$ and $\Gamma \sim O(1)$

β	$\mathrm{Im}[c^{(1)}_{\mathrm{elas}}]$	$\mathrm{Im}[c^{(1)}_{\mathrm{visc}}]$	$\mathrm{Im}[c^{(1)}_{\mathrm{solid}}]$
0.2	$0.013(W_b - 1.148W_a)$	$-7.7 \times 10^{-5} Re$	$0.07\Gamma H(H^2 + 2H + 1.25)$
0.4	$0.0008(W_a - 3.94W_b)$	$-4.8 \times 10^{-5} Re$	$0.007\Gamma H(H + 1.03)(H + 8.92)$
0.5	$0.014(W_a - 1.21W_b)$	$1.43 \times 10^{-6} Re$	$-0.04306(H + 0.862)(H - 0.865)$
0.6	$0.018(W_a - 1.13W_b)$	$6 \times 10^{-5} Re$	$-0.0685\Gamma H(H + 0.738)(H + 0.019)$
0.8	$0.0099(W_a - 1.08W_b)$	$8.9 \times 10^{-5} Re$	$-0.038\Gamma H(H^2 + 1.11H + 0.366)$

It is well recognized that this shooting procedure needs a good initial guess in order to converge to the desired eigenvalue. For this purpose, we use the results from our low-k asymptotic analysis in the previous section as starting guesses, and continue the low-k results numerically to finite k for the two-fluid interfacial mode. For the fluid B–solid interfacial mode, we use results from a zero-Re analysis for the present three layer configuration (which gives analytical solutions for the wavespeed) for $\mu_r = 1$, and we numerically continue these results to finite Re and desired μ_r. We have validated our numerical procedure and computer code by comparing our results to a variety of previous studies: firstly, we set $\mu_r = 1$, $\Gamma = 0$ and $W_a = W_b \neq 0$, and compare the results from our numerical solutions with that of Renardy and Renardy [25] who used a spectral method to calculate the stable modes of UCM plane Couette flow in a rigid channel. Secondly, we set $\mu_r = 1$, $W_a = W_b$ but $\Gamma \neq 0$, and compare the present results with that of Shankar and Kumar [14] who provided analytical solutions for the stability of single layer UCM Couette flow past a deformable wall. We have also compared the present results when $\Gamma = 0$ with that of Yih[17] (two-layer Newtonian plane Couette flow) and Chen [2] (two-layer UCM plane Couette flow) in the limit $k \ll 1$. Finally, we have also compared the results from our numerical code with the asymptotic results of the previous section in the $k \ll 1$ limit. Excellent agreement was found in all these comparisons. We now turn to the discussion of the results obtained from the numerical method.

4.2. Results

In all the numerical results discussed below, the Reynolds number Re is set to 1 without loss of generality. As remarked in our discussion on the results from asymptotic analysis in Section 3, when $Re \sim O(1)$, it does not play a very significant role compared to the destabilizing contribution due to elasticity stratification. Therefore, all the qualitative conclusions drawn below from the results with $Re = 1$ are expected to be valid for other values of $Re \sim O(1)$. We first show in Fig. 2 the variation of c_i with k for two-layer flow with and without the deformable solid layer in order to demonstrate the effect of solid layer deformability on the two-fluid interfacial mode. Fig. 2(a) shows the variation of c_i versus k when the non-dimensional interfacial tension Σ is set to zero. For the case of two-layer flow in a rigid channel (i.e. in the absence of the deformable solid layer, which is mimicked here by setting $\Gamma \to 0$), the two-fluid interfacial mode is unstable at all wavenumbers for the configuration considered in Fig. 2(a), and the most unstable waves are the ones with $k \sim O(1)$. When $\Gamma = 1.5$, the solid layer deformability stabilizes the two-fluid interfacial instability due to elasticity stratification in the low wavenumber limit. The numerical results show that the stabilizing effect predicted by the low-k asymptotic analysis extends to intermediate values of $k \simeq 1$. For $k > 2$, however, the system again becomes unstable and for higher values of k, the two curves for $\Gamma = 0$ and $\Gamma = 1.5$

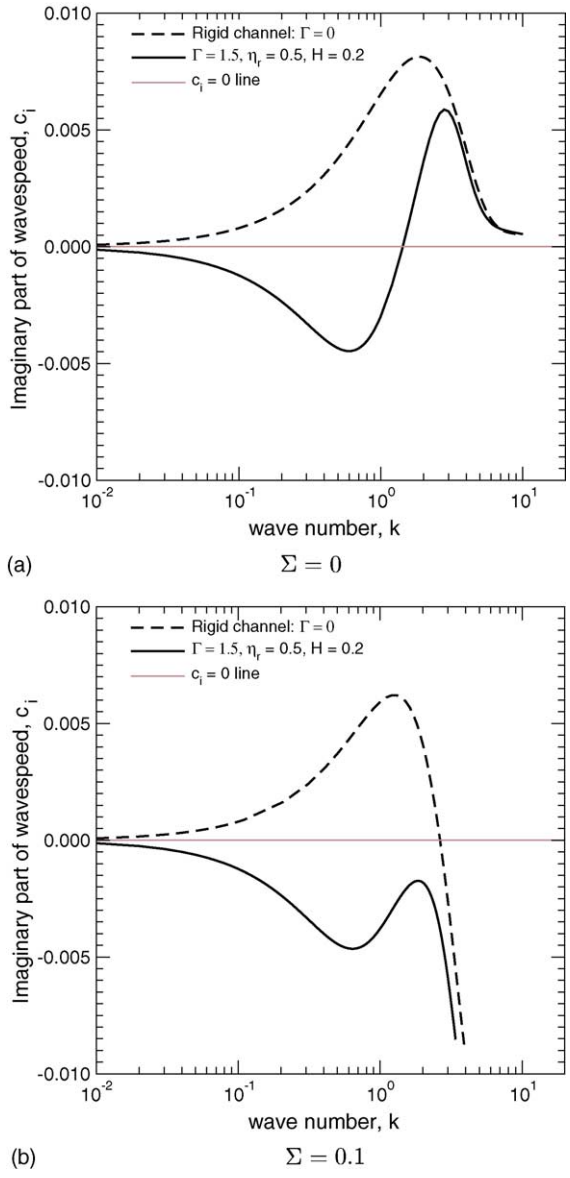

Fig. 2. Stabilization of the two-fluid interfacial mode by the deformable solid layer, while it is unstable in a rigid channel: c_i vs. k for $W_a = 0.5$, $W_b = 1$, $\beta = 0.4$, $\mu_r = 0.5$, $Re = 1$ for $\Sigma = 0$, and $\Sigma \neq 0$.

coincide with each other. This implies that the solid layer deformability has no effect on the high-k perturbations, because the fluid velocity perturbations are localized near the two-fluid interface for these short wavelength fluctuations. Such high-k unstable perturbations can be stabilized only by the presence of a sufficiently strong non-zero interfacial tension between the two fluids. Fig. 2(b) shows the effect of non-zero Σ on the two-fluid interfacial mode both for $\Gamma = 0$ and $\Gamma = 1.5$. These data demonstrate that in the presence of a sufficiently strong interfacial tension, the two-fluid interfacial instability is completely stabilized at all wavenumbers by the deformable solid layer.

In Fig. 3, we show the results for a configuration which is identical to that shown in Fig. 2(b), except for μ_r, which

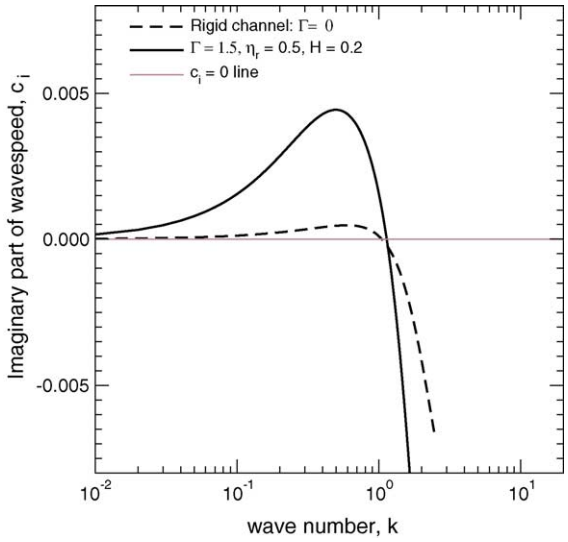

Fig. 3. Destabilization of the two-fluid interfacial mode by the deformable solid layer: c_i vs. k for $W_a = 0.5$, $W_b = 1$, $\beta = 0.4$, $Re = 1$, $\Sigma = 0.1$, and $\mu_r = 1.5$.

increased to 1.5, keeping W_a and W_b same as before. As remarked in Section 3, the fluid viscosity ratio μ_r crucially controls the stabilizing or destabilizing nature of the deformable solid layer on the two-fluid interfacial mode. The data shown in Fig. 3 shows that merely by increasing μ_r from 0.5 to 1.5, the deformable solid layer becomes completely destabilizing, when compared to the stabilizing effect shown in Fig. 2(b). For the data shown in Fig. 3, the two-fluid interfacial mode is unstable even in the absence of the solid layer. However, the presence of the solid layer increases the magnitude of c_i, thus rendering the two-fluid interfacial mode more unstable. Fig. 4 shows the destabilizing nature of the deformable solid for the case where the two-fluid mode is stable in a rigid channel in the low wavenumber limit. Fig. 4(a) shows the data for the case with zero interfacial tension between the two fluids. For this configuration, while the two-fluid interfacial mode is stable in a rigid channel in the limit of low and intermediate wavenumbers, it becomes unstable for $k \simeq 10$. These high-k unstable perturbations are similar to those predicted by Renardy [1], who used a short-wave asymptotic analysis and showed that the two-layer flow of UCM fluids with elasticity stratification is always unstable in the absence of interfacial tension between the two fluids. Fig. 4(a) shows that the solid layer deformability renders the two-fluid mode unstable in the low-k-limit, but as k increases, the flow becomes stable. For very large k, the curves for both $\Gamma = 0$ and $\Gamma = 1$ sco-incide, indicating that the solid layer has no effect on these high-k perturbations. Fig. 4(b) shows the data for the same configuration, but with non-zero interfacial tension.

While the above discussion in terms of c_i versus k for a specified value of Γ illustrates the stabilizing and destabilizing nature of the solid layer, it is useful to construct neutral stability curves (curves with $c_i = 0$) in the Γ–k plane for fixed values of other parameters W_a, W_b, μ_r, β, H, and Σ. These

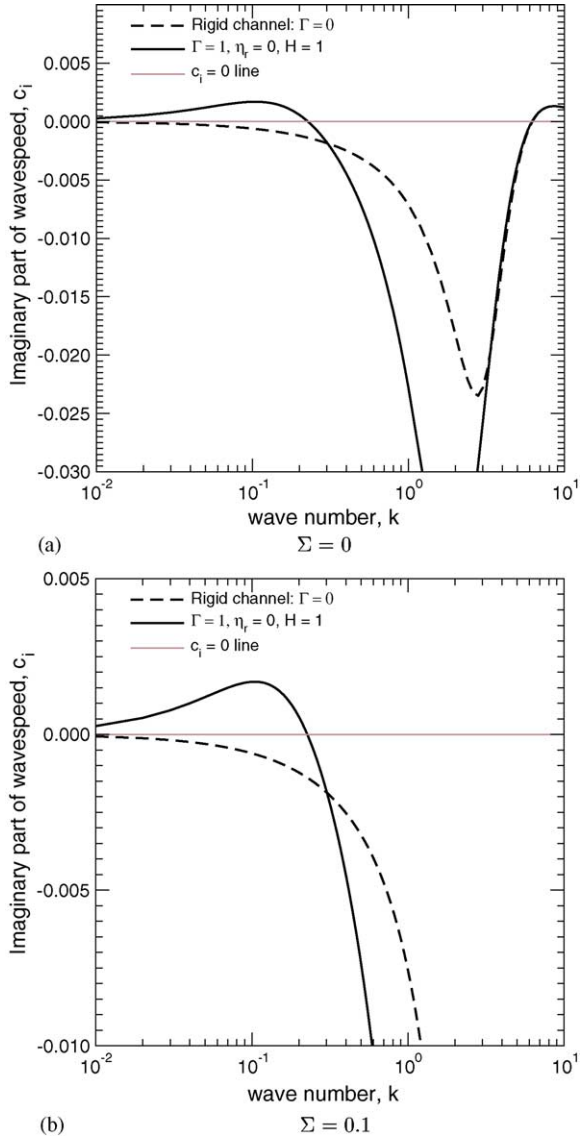

Fig. 4. Destabilization of the two-fluid interfacial mode by the deformable solid layer while it is stable in a rigid channel: c_i vs. k for $W_a = 0.5$, $W_b = 1$, $\beta = 0.7$, $Re = 1$, and $\mu_r = 0.5$ for $\Sigma = 0$ and $\Sigma \neq 0$.

plots will allow us to choose the parameter $\Gamma = V\mu_b/(GR)$ (which is a non-dimensional measure of the shear modulus of the solid layer) so that the two-fluid interfacial mode is stabilized. Also, at finite k, the interfacial mode between fluid B and the solid layer could become unstable when Γ becomes sufficiently high. Thus, when neutral stability curves are constructed for both the interfacial modes in the Γ–k plane, this will allow us to demarcate the regions in which both the interfacial modes are stable. In the ensuing discussion, we only present data with $\Sigma \neq 0$, so that the unstable high-k fluctuations of the two-fluid interfacial mode are always stabilized. The low-k asymptotic analysis indicated that the solid to fluid viscosity ratio η_r does not come into play in the $k \ll 1$ limit. However, for $k \sim O(1)$, η_r was found to have a stabilizing effect both on the two-fluid interfacial mode as well as the fluid

B–solid interfacial mode. Therefore, we have also considered non-zero values of η_r in the results presented below. For ease of discussion of the figures, we designate the two-fluid interfacial mode due to elasticity and viscosity stratification as 'mode 1', and the fluid B–solid interfacial mode as 'mode 2'.

Figs. 5(a) and (b) show the neutral stability curve for the two-fluid interfacial mode in the presence of the solid layer in the Γ–k plane for different values of μ_r. Note that $\Gamma = 0$ is the limit of a rigid solid layer, and for the configuration chosen in these plots, the two-fluid interfacial mode is unstable in a rigid channel. As Γ is increased, the two-fluid interfacial instability is stabilized by the deformable solid when the neutral stability curve is crossed, and unstable and stable domains are marked in the respective figures. When $\mu_r \neq 1$, the Γ required to stabilize the two-fluid interfacial instability remains an $O(1)$ quantity at low and intermediate values of k. At high values of k, the interfacial tension between the two fluids stabilizes the instability. These figures also demonstrate the important difference between the behaviour for $\mu_r \neq 1$ and $\mu_r = 1$. When $\mu_r = 1$, $\Gamma \propto k^{-1}$ for $k \ll 1$, in marked contrast with the curves with $\mu_r \neq 1$. Even a small deviation from $\mu_r = 1$ to $\mu_r = 0.9$ is sufficient to change the scaling from $\Gamma \propto k^{-1}$ to $\Gamma \sim O(1)$ in the $k \ll 1$ limit. Also, as μ_r deviates further from 1, the Γ value required to stabilize the two-fluid interfacial instabil-

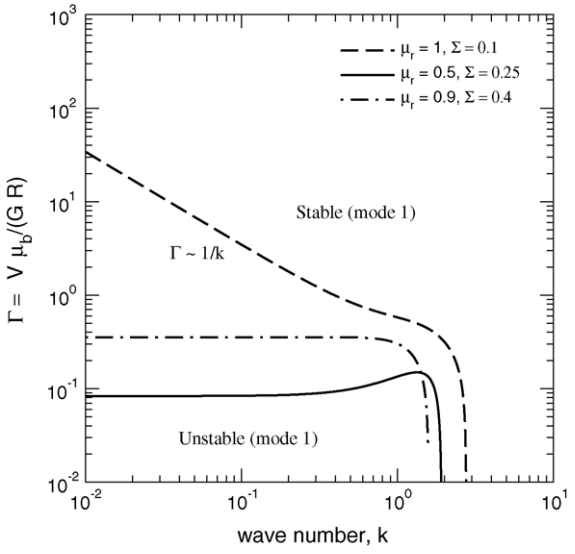

(a) $W_a = 0.1, W_b = 0.5, Re = 1, \beta = 0.4, H = 0.7, \eta_r = 0.6$

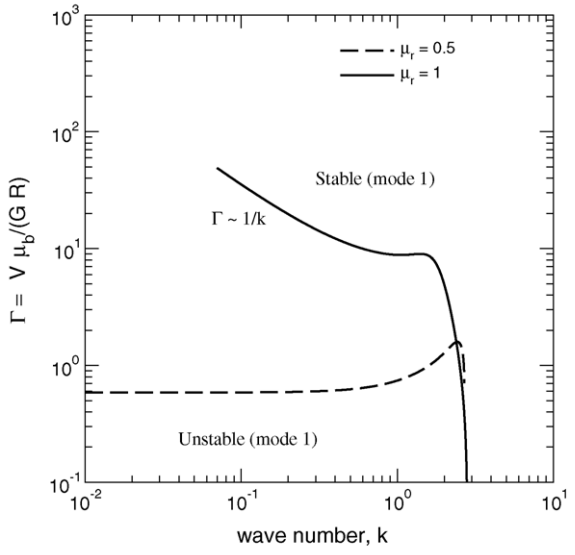

(b) $W_a = 0.5, W_b = 1, Re = 1, \beta = 0.4, H = 0.2, \eta_r = 0, \Sigma = 0.1$.

Fig. 5. Neutral stability curve in the Γ–k plane: effect of μ_r on the stabilization of the two-fluid interfacial mode by solid layer deformability.

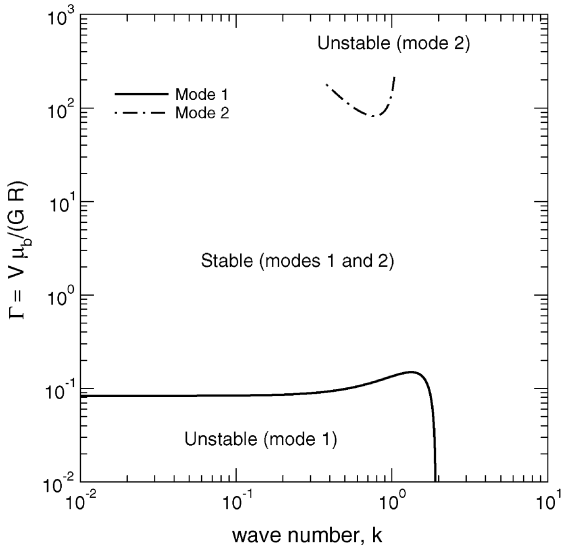

(a) $W_a = 0.1, W_b = 0.5, Re = 1, \mu_r = 0.5, \beta = 0.4, H = 0.7, \eta_r = 0.6, \Sigma = 0.25$.

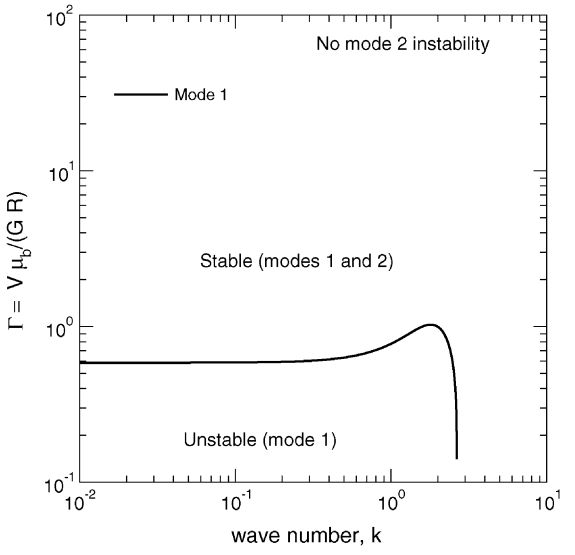

(b) $W_a = 0.5, W_b = 1, Re = 1, \mu_r = 0.5, \beta = 0.4, H = 0.2, \eta_r = 0.5, \Sigma = 0.1$.

Fig. 6. Neutral stability curves in the Γ–k plane for the two-fluid interfacial mode (mode 1) and the fluid–solid interfacial mode (mode 2): stabilization of the two-fluid interfacial mode by solid layer deformability.

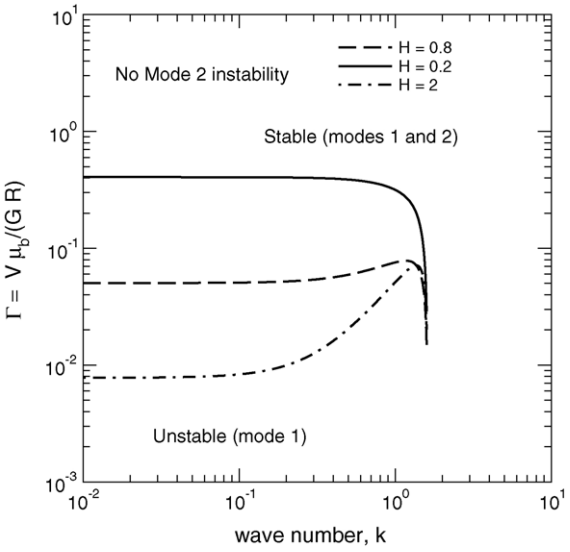

Fig. 7. Effect of solid layer thickness H on the stabilization of two-fluid interfacial instability by the deformable solid layer: neutral stability curves in the Γ–k plane. Data for $W_a = 1$, $W_b = 2$, $Re = 1$, $\mu_r = 0.25$, $\beta = 0.4$, $\eta_r = 1$, $\Sigma = 0.1$.

ity also decreases substantially. From a practical viewpoint, this result implies that when $\mu_r \neq 1$, the Γ values required to stabilize the two-fluid interfacial mode are much smaller than that for $\mu_r = 1$. Since $\Gamma = V\mu_b/(GR)$, a smaller Γ implies a larger shear modulus of the elastic solid layer, so deformable solids with significantly larger shear modulii can be used to stabilize the two-fluid interfacial instability when $\mu_r \neq 1$.

Fig. 6(a) shows the stabilization of the two-fluid interfacial mode (mode 1) by the solid layer, along with the neutral curve for the fluid B–solid interfacial mode (mode 2). As the solid layer is made deformable, i.e. as Γ is increased, we first encounter the neutral curve for mode 1. As Γ crosses this curve, mode 1 instability is stabilized by the solid layer. There is then a wide range of Γ values in which both mode 1 and mode 2 are stable. When Γ is increased beyond a large value, the fluid B–solid layer interfacial mode becomes unstable. However, there is a wide window in the parameter Γ (or, equivalently, the shear modulus of the solid) in which both the interfacial modes are stable. In Fig. 6(b), we again demonstrate the suppression of mode 1 by the solid layer deformability. However, in this case there is no mode 2 instability for the given set of W_a, W_b, and H. Fig. 7 shows the effect of the solid layer thickness H on the neutral curves in the Γ–k plane for the mode 1 instability. For small k, the Γ value required to stabilize the two-fluid unstable mode decreases with increase in H (see Eq. (43) for an illustration from the low-k asymptotic results). However, for finite k, the Γ values required to stabilize increases with k for $H = 2$, while for $H = 0.8$, it remains approximately constant. For $H = 0.2$, however, the Γ value required is much larger than that for the other two data. A larger Γ implies (with all other parameters being the same) a solid layer with a lower shear modulus G. However, if it is desired to have a solid with larger shear modulus, it is necessary to choose a solid layer with larger thickness. Also, in order to suppress the two-fluid instability completely, it is necessary to stabilize waves with all wavenumbers, and so an optimum solid layer thickness H can be chosen for which the Γ–k curve is relatively flat ($H = 0.8$ is a good candidate in this particular instance).

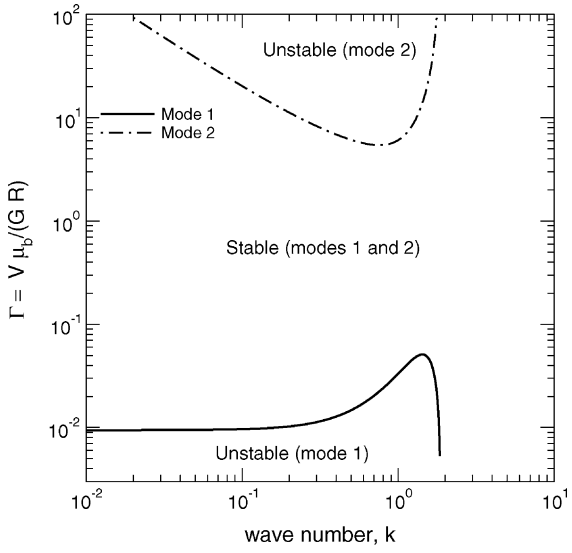

(a) $W_a = 2$, $W_b = 1$, $Re = 1$, $\mu_r = 5$, $\beta = 0.7$, $H = 1$, $\eta_r = 0$, $\Sigma = 0.5$.

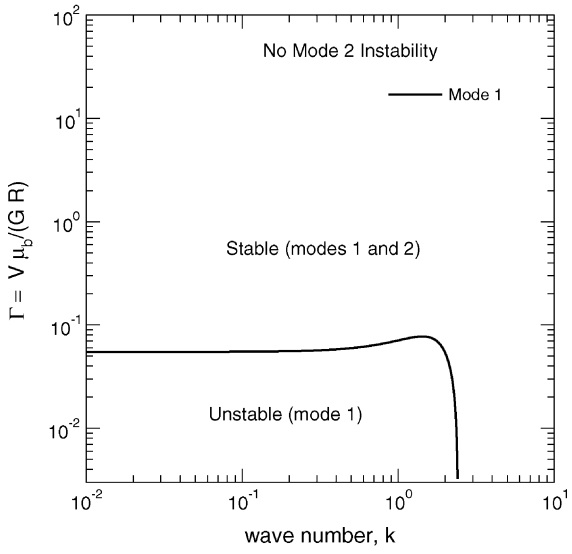

(b) $W_a = 0.5$, $W_b = 0.1$, $Re = 1$, $\mu_r = 4$, $\beta = 0.8$, $H = 0.5$, $\eta_r = 1$, $\Sigma = 0.5$.

Fig. 8. Neutral stability curves in the Γ–k plane for the two-fluid interfacial mode and the fluid–solid interfacial mode: stabilization of the two-fluid interfacial mode by solid layer deformability.

Our discussion thus far has centered around demonstrating the stabilizing nature of the solid layer at low and finite k. For the configurations discussed above, the stabilizing nature of the solid layer is not altered even if $\mu_r = 1$, except for the change in the Γ–k neutral curve for small k (discussed in Fig.

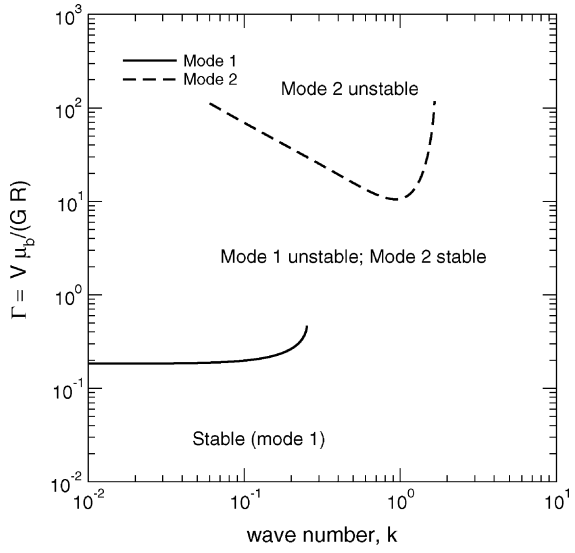

(a) $W_a = 0.5, W_b = 1, Re = 1, \mu_r = 0.5, \beta = 0.7, H = 1, \eta_r = 0, \Sigma = 0.$

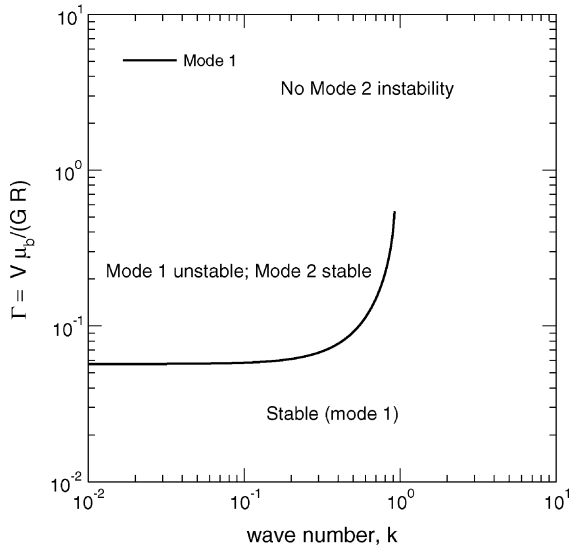

(b) $W_a = 0.5, W_b = 1, Re = 1, \mu_r = 2, \beta = 0.4, H = 0.5, \eta_r = 0, \Sigma = 0.1.$

Fig. 9. Neutral stability curves in the Γ–k plane for the two-fluid interfacial mode and the fluid–solid interfacial mode: destabilization of the two-fluid interfacial mode by solid layer deformability.

5). We now present data for the case where the solid layer has a destabilizing effect if $\mu_r = 1$ according to the results of the earlier study [16], but with the presence of viscosity contrast $\mu_r \neq 1$, the nature of the solid layer becomes stabilizing. This is shown in Fig. 8. These figures show that by tuning the viscosity ratio μ_r it is possible to completely stabilize the two-fluid interfacial instability by the deformable solid layer. Finally, in Fig. 9, we show the destabilizing nature of the solid layer on the two-fluid interfacial mode while it is stable in the absence of the solid layer. In this case, as Γ is increased from zero, when the mode 1 neutral curve is crossed, the two-fluid interfacial mode is destabilized first. When Γ is increased further, mode 2 is destabilized next by the deformable solid layer. These results, thus, demonstrate that by tuning the shear modulus of the solid layer, viscosity ratio between the two fluids, and the viscosity ratio between the fluid and the solid, it is possible to completely suppress or induce two-fluid interfacial instabilities due to elasticity and viscosity stratification.

In the present study, we had used the linear viscoelastic model to describe the deformation in the solid layer. In principle, one might expect the linear elastic model to be valid only when the non-dimensional strain in the base state of the solid layer (Eq. (13)) is small compared to unity. In our earlier study [16], we had used the neo-Hookean model to describe the solid layer (also see [23]) in order to examine the consequences of using a non-linear model for the solid, and compared the results with the results obtained from the linear viscoelastic solid model. It was found that the neutral curves were not altered significantly for the two-fluid interfacial mode due to elasticity stratification, and all the qualitative features for both the neo-Hookean and the linear viscoelastic solid model remained the same. The non-dimensional strain in the base state of the solid layer is proportional to the parameter Γ. For the results presented in this paper, the non-dimensional parameter $\Gamma \sim 10^{-1}$ for achieving the stabilization or destabilization of the two-fluid interfacial mode. Since the Γ required to realize these effects is small compared to unity, the present predictions for stabilization/destabilization of the two-fluid interfacial mode are expected to be accurate despite the use of a simple linear viscoelastic solid model to describe the deformable solid layer.

5. Concluding remarks

In conclusion, the present study concerning the stability of two-layer viscoelastic plane Couette flow past a deformable solid layer shows that the viscosity difference between the two fluids has a profound impact on the stabilization of the two-fluid interfacial instability due to elasticity and viscosity stratification by the deformable solid layer. The effect of solid layer deformability on the two-fluid interfacial mode was first examined using a low wavenumber asymptotic analysis. Results from our analysis showed that the effect of the deformable solid layer appeared at $O(k)$ in the asymptotic expansion for the wavespeed, the same order at which the elasticity stratification term and viscosity stratification term appeared. These three contributions can be stabilizing or destabilizing in the low wavenumber limit, depending on W_a, W_b, μ_r, β, Γ, and H. Our asymptotic results showed that the stabilizing or destabilizing nature of the solid layer is determined by the fluid viscosity ratio μ_r and the solid elasticity parameter Γ, and is independent of the relaxation times of the two fluids W_a and W_b. This conclusion is a significant departure from the results of the earlier study [16] obtained for the special case of matched fluid viscosities $\mu_r = 1$. In general,

it is found that the solid layer has a stabilizing effect when $\mu_r < 1, \beta < 0.5$ and $\mu_r > 1, \beta > 0.5$, while it could have both destabilizing or stabilizing effects (depending on H and β) when $\mu_r < 1, \beta > 0.5$ and $\mu_r > 1, \beta < 0.5$. The two-fluid interfacial mode due to elasticity and viscosity stratification is unstable or stable (in the absence of the solid layer) depending on W_a, W_b, μ_r, and β. Thus, under appropriate combinations of W_a, W_b, μ_r, β, and the solid elasticity parameter Γ, the two-fluid interfacial mode can be stabilized (destabilized) by making the solid layer deformable while it is unstable (stable) in the absence of the solid layer.

Another important result from the present asymptotic analysis is that in the limit of low k, when $\mu_r \neq 1$, the solid elasticity parameter $\Gamma \sim O(1)$ in order for the solid layer to have an effect on the two-fluid interfacial mode. In stark contrast, $\Gamma \propto k^{-1}$ in the $k \ll 1$ limit for the case of matched fluid viscosities $\mu_r = 1$ considered in the earlier study [16]. This implies that the configuration with matched fluid viscosities must be viewed as a special case insofar as the effect of the solid layer is concerned, and even minor viscosity differences between the two fluids can qualitatively change the low-k scaling of the neutral curve in the Γ–k plane. Furthermore, for $\mu_r \neq 1$, the numerical values of the non-dimensional parameter Γ are significantly smaller than unity in order to achieve stabilization of the two-fluid interfacial mode. As a consequence, when the viscosities of the two UCM fluids are different, the non-dimensional solid elasticity parameter Γ required for stabilization is much smaller compared to the case with matched viscosities, meaning solids with significantly larger shear modulii could be used to suppress the two-fluid interfacial instabilities in viscoelastic fluids with viscosity mismatch. The results of our low wavenumber asymptotic analysis were continued to finite and large values of k by numerically solving the stability equations governing the present three-layer configuration. The numerical results at finite k revealed that while the predicted stabilization at low-k extends to intermediate values of $k \sim O(1)$, at high values of k the solid layer has no effect on the two-fluid interfacial mode. These high-k unstable waves are stabilized by the presence of a sufficiently strong interfacial tension between the two fluids. Neutral stability curves for the interfacial mode between fluid B and the solid layer were also constructed (for cases when the fluid–solid interfacial instability is present) and it was shown that there exists a significant window in the parameter Γ in which both the interfacial modes are stable.

Finally, it is useful to estimate the various non-dimensional parameters in order to determine when the present predictions can be realized in typical experimental situations. To this end, we choose the low wavenumber asymptotic result for Γ (Eq. (43)) for $W_a = 1$, $W_b = 2$, $\beta = 0.4$, and $\mu_r = 0.5$. For $H = 1$, $\Gamma_0 \simeq 0.097$ from Eq. (43) for the system to be neutrally stable (assuming $Re \sim O(1)$). When $\Gamma > 0.097$, the two-fluid interfacial instability due to elasticity stratification is stabilized by the deformability of the solid layer in the low wavenumber limit. Numerical results show that even at finite k, the system is stable if $\Gamma > 0.097$. Since $W_b = 2$, the ratio $\Gamma/W_b > 0.048$ for achieving stabilization by the solid layer. This non-dimensional ratio $\Gamma/W_b = \mu_b/(G\tau_b)$ is independent of the fluid velocity V, and when $\mu_b/(G\tau_b) > 0.048$, the interfacial instability due to elasticity stratification will be stabilized. (The fluid velocity V serves to determine only the Reynolds number, and Re is assumed to be at most $O(1)$ here.) Since $W_b > W_a$, Γ/W_a is also greater than 0.048. The shear modulus G of soft elastomeric solids can be estimated to be around 10^5 Pa, while the viscosity and relaxation time for typical polymeric fluids are estimated to be 10^2 N s m^{-2} and 10^{-2} s, respectively. Using these typical estimates the non-dimensional group $\mu_b/(G\tau_b) = 0.1$ and this is clearly greater than 0.048 required for stabilization. These approximate estimates thus suggest that the predicted stabilization can be potentially realized in experiments involving two-layer flows of typical polymeric liquids past soft elastomeric solid layers.

References

[1] Y. Renardy, Stability of the interface in two-layer Couette flow of upper convected Maxwell liquids, J. Non-Newtonian Fluid Mech. 28 (1988) 99–115.

[2] K. Chen, Elastic instability of the interface in Couette flow of two viscoelastic liquids, J. Non-Newtonian Fluid Mech. 40 (1991) 261–267.

[3] Y.-Y. Su, B. Khomami, Purely elastic interfacial instabilities in superposed flow of polymeric fluids, Rheol. Acta 31 (1992) 413–420.

[4] Y.-Y. Su, B. Khomami, Interfacial stability of multilayer viscoelastic fluids in slit and converging channel die geometries, J. Rheol. 36 (1992) 357–387.

[5] G.M. Wilson, B. Khomami, An experimental investigation of interfacial instabilities in the multilayer flow of viscoelastic fluids Part I. Incompatible polymer systems, J. Non-Newtonian Fluid Mech. 41 (1992) 355.

[6] G.M. Wilson, B. Khomami, An experimental investigation of interfacial instabilities in the multilayer flow of viscoelastic fluids Part II. Elastic and non-linear effects in incompatible polymer systems, J. Rheol. 37 (1993) 315.

[7] G.M. Wilson, B. Khomami, An experimental investigation of interfacial instabilities in the multilayer flow of viscoelastic fluids Part III. Compatible polymer systems, J. Rheol. 37 (1993) 341.

[8] B. Khomami, G.M. Wilson, An experimental investigation of interfacial instabilities in the superposed flow of viscoelastic fluids in converging/diverging channel geometry, J. Non-Newtonian Fluid Mech. 58 (1995) 47.

[9] H.J. Wilson, J.M. Rallison, Short wave instability of co-extruded elastic liquids with matched viscosities, J. Non-Newtonian Fluid Mech. 72 (1997) 237–251.

[10] H. Ganpule, B. Khomami, A theoretical investigation of interfacial instabilities in the three layer superposed channel flow of viscoelastic fluids, J. Non-Newtonian Fluid Mech. 79 (1998) 315–360.

[11] H. Ganpule, B. Khomami, An investigation of interfacial instabilities in the superposed channel flow of viscoelastic fluids, J. Non-Newtonian Fluid Mech. 81 (1999) 27–69.

[12] S. Scotto, P. Laure, Linear stability of three-layer poiseuille flow for Oldroyd - B fluids, J. Non-Newtoian Fluid Mech. 83 (1999) 71–92.

[13] V. Kumaran, G.H. Fredrickson, P. Pincus, Flow induced instability of the interface between a fluid and a gel at low Reynolds number, J. Phys. II France 4 (1994) 893–904.

[14] V. Shankar, S. Kumar, Instability of viscoelastic plane Couette flow past a deformable wall, J. Non-Newtonian Fluid Mech. 116 (2004) 371–393.

[15] V. Kumaran, R. Muralikrishnan, Spontaneous growth of fluctuations in the viscous flow of a fluid past a soft interface, Phys. Rev. Lett. 84 (2000) 3310–3313.
[16] V. Shankar, Stability of two-layer viscoelastic plane Couette flow past a deformable solid layer, J. Non-Newtonian Fluid Mech. 117 (2004) 163–182.
[17] C.S. Yih, Instability due to viscosity stratification, J. Fluid. Mech. 27 (1967) 337–350.
[18] V.A. Gorodtsov, A.I. Leonov, On a linear instability of plane parallel Couette flow of viscoelastic fluid, J. Appl. Math. Mech. 31 (1967) 310–319.
[19] V. Shankar, L. Kumar, Stability of two-layer Newtonian plane Couette flow past a deformable solid layer, Phys. Fluids 16 (2004) 4426–4442.
[20] R.G. Larson, Constitutive Equations for Polymer Melts and Solutions, Butterworths, Boston, 1988.
[21] V. Shankar, V. Kumaran, Stability of non-parabolic flow in a flexible tube, J. Fluid Mech. 395 (1999) 211–236.
[22] V. Shankar, V. Kumaran, Stability of fluid flow in a flexible tube to non-axisymmetric disturbances, J. Fluid Mech. 408 (2000) 291–314.
[23] V. Gkanis, S. Kumar, Instability of creeping Couette flow past a neo-Hookean solid, Phys. Fluids 15 (2003) 2864–2871.
[24] P. Drazin, W. Reid, Hydrodynamic Stability, Cambridge University Press, Cambridge, 1981.
[25] M. Renardy, Y. Renardy, Linear stability of plane Couette flow of an upper convected Maxwell fluid, J. Non-Newtonian Fluid Mech. 22 (1986) 23–33.